Materials Science and Engineering A 393 (2005) 133–139

MATERIALS SCIENCE & ENGINEERING A

www.elsevier.com/locate/msea

Elastic properties of ceramic–metal particulate composites

C.L. Hsieh, W.H. Tuan*

Department of Materials Science and Engineering, National Taiwan University, Taipei, Taiwan

Received 12 July 2004; received in revised form 1 October 2004; accepted 6 October 2004

Abstract

In the present study, the experimental data on the elastic properties of several ceramic–metal systems, Al_2O_3–NiAl, SiC–Al, WC–Co and glass–W, are compiled and compared with several theoretical predictions. These theoretical predictions offer upper and lower bounds on the elastic constants. The elastic moduli of the ceramic–metal composites fall well within the Voigt–Reuss bounds and Hashin–Shtrikman (H–S) bounds. Though most the Poisson's ratio of ceramic–metal composites falls within the modified H–S bounds, the values of the composites with low second-phase concentration deviate from model predictions. The deviation shows strong dependence on the interconnectivity of each phase in the composites.

Keywords: Composites; Elastic modulus; Poisson's ratio

1. Introduction

The elastic properties of monolithic materials (ceramics or metals) depend strongly on their bonding characteristics [1]. For example, the elastic modulus of monolithic ceramics reflects their cation-oxygen bonding length and strength under tension [2]. The bending strength of inter-atomic bonds determines the magnitude of shear modulus. Among these elastic constants, Koester and Franz suggested that the Poisson's ratio provided more information about the character of the bonding forces [3]. Furthermore, the elastic constants are sensitive to the composition change. The presence of solute can alter the bonding characteristics as well as the elastic constants of materials [2].

The bonding characteristics of ceramics are different from those of metal. The addition of ceramic into metal or vice versa introduces heterogeneous interfaces. To be demonstrated later, the elastic properties of the two-phase materials often deviate from the prediction made by using the rule of mixtures. It may be related to the presence of heterogeneous interface.

Though the properties of ceramics and metals are different, the combination of two materials to form composite exhibits many potential applications. For example, the hardness of tungsten carbide (WC) is very high; nevertheless, the sintering between WC particles is not possible below 1500 °C. Metallic cobalt can bond WC particles strongly together at a relatively low temperature [4]. The WC–Co composite can thus be applied as cutting tool. The addition of Al into SiC can result in improved thermal stability [5]. The addition of NiAl improves the toughness of Al_2O_3 [6]; the presence of ZrO_2 particles enhances the high temperature strength of NiAl [7].

The knowledge about the elastic properties of two-phase systems is essential for designing new composites and functionally graded materials [8–13]. With the knowledge of the elastic modulus, other properties such as hardness and creep resistance can then be estimated [14,15]. There are many theoretical models available to predict the elastic constants of two-phase materials [16–38]. Some models contain one or two adjustable variables that have to be determined experimentally [19–23,25–38]. Some models need only the properties of the two constituents to predict the elastic constants [8,16–18,24]. Among these models, several models can offer fixed values for the elastic properties of two-phase materials [8,19–21]. Several models propose upper and lower bounds instead [8,16,17,19–21,32–36]. All these models claim that

* Corresponding author. Tel.: +886 2 23659800; fax: +886 2 23634562.
E-mail address: tuan@ccms.ntu.edu.tw (W.H. Tuan).

0921-5093/$ – see front matter
doi:10.1016/j.msea.2004.10.009

they can match the experimental data well. However, the pre-existed experimental data cover only part of the composition range for a certain composite. A recent study reported the elastic constants of Al_2O_3-NiAl system for whole range of composition [37], which makes comparison between experimental data and theoretical predictions possible. Apart from the data of Al_2O_3–NiAl system, the available data for other ceramic–metal composites, SiC–Al, WC–Co and glass–W, are also compared in the present study to verify the model predictions.

2. Theoretical models

Most theoretical models are made under the assumptions of perfect bonding at the interface, strain compatible and negligible elastic interaction between particles [16–38]. These models further employed simplified geometries, as shown in Fig. 1, to derive their mathematical equations. In the present study, experimental data are compared with the theoretical predictions. A comprehensive data collection on the ceramic–metal composites has been carried out. These experimental data vary within a range instead of a specific point. The model predictions that can provide upper and lower bounds to cover the experimental data seem more plausible. Therefore, the following three models are chosen: (1) Voigt–Reuss, (2) Hashin–Shtrikman (H–S) and (3) Ravichandran models.

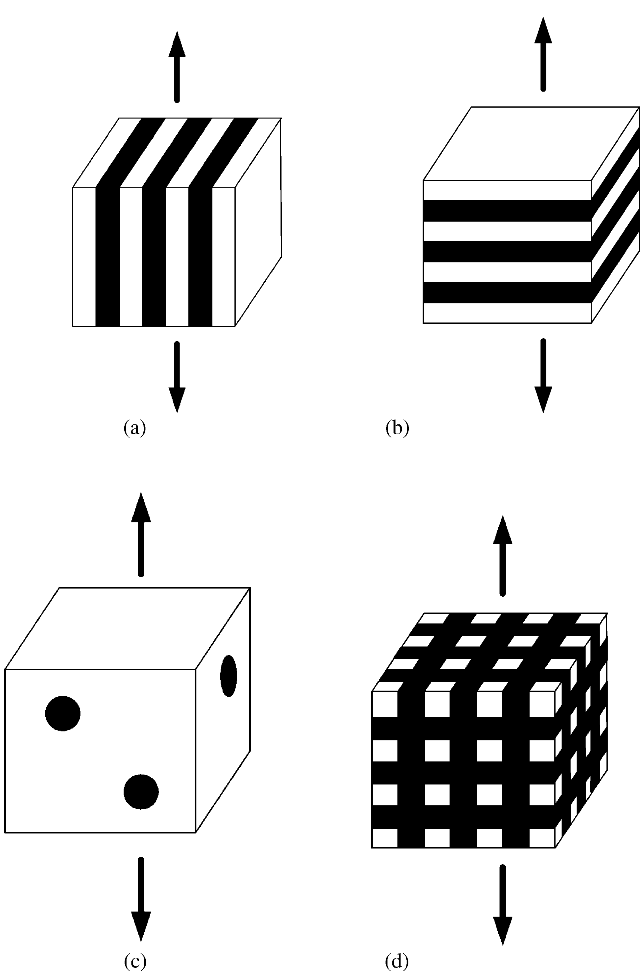

Fig. 1. The unit cell proposed in (a) iso-strain (Voigt) state and (b) iso-stress (Reuss) state. The geometrical models employed by (c) Hashin–Shtrikman (H–S) and (d) Ravichandran models. The arrows indicate the direction of the external load.

2.1. Voigt–Reuss bounds

Fig. 1(a) shows the case that the strain of the two phases in the composite under an external load is the same. The loading direction is parallel to the interface. The elastic modulus of the composite, E_c, as proposed by Voigt [16] is

$$E_c^u = E_m V_m + E_p V_p \tag{1}$$

with $V_m + V_p = 1$, V_m and V_p are the volume fraction of matrix and particle, respectively. Eq. (1) follows the rule of mixtures. When the composite is under an iso-stress state as proposed by Reuss [17], as shown in Fig. 1(b), the elastic modulus is expressed as

$$E_c^l = \frac{E_m E_p}{E_m V_p + E_p V_m} \tag{2}$$

The superscripts u and l denote upper and lower bounds, respectively. As pointed out by Hill [22], neither iso-strain nor iso-stress assumption is realistic. The tractions at interface are not at equilibrium under the Voigt condition; the interface could not remain bonded under the Reuss condition. Though the equality in Eq. (1) is true only when the Poisson's ratios of the two phases are the same; the values predicted by Eqs. (1) and (2) are widely treated as the upper and lower bounds of the elastic modulus of any two-phase materials, respectively [5]. The Voigt–Reuss bounds are thus used in the present study to compare the experimental data.

Each value of elastic modulus (E), shear modulus (G), bulk modulus (K) and Poisson's ratio (ν) can be calculated by knowing any two elastic constants. However, it should be noted that it is not suitable to calculate the Poisson's ratio under the iso-strain and iso-stress assumptions.

2.2. Hashin–Shtrikman (H–S) bounds

Hashin and Shtrikman treated the two-phase system composing of one randomly distributed particulate phase and one continuous matrix phase, Fig. 1(c). The model provides bounds for the elastic constants of a two-phase material with a random isotropic distribution of phases from the properties and volume fraction of each phase [19–21,36]. The "minimum energy" principle was employed to show the bounds on the bulk modulus and shear modulus as

$$K_C^l = K_m + \frac{V_p}{(1/K_p - K_m) + (3V_m/3K_m + 4G_m)} \tag{3}$$

$$K_C^u = K_p + \frac{V_m}{(1/K_m - K_p) + (3V_p/3K_p + 4G_m)} \quad (4)$$

$$G_C^l = G_m + \frac{V_p}{(1/G_p - G_m) + (6(K_m + 2G_m)V_m/5G_m(3K_m + 4G_m))} \quad (5)$$

$$G_C^u = G_p + \frac{V_m}{(1/G_m - G_p) + (6(K_p + 2G_p)V_p/5G_p(3K_p + 4G_p))} \quad (6)$$

The lower and upper bounds on the elastic modulus can be estimated by using the following equations as

$$E_c^l = \frac{9K_c^l G_c^l}{3K_c^l + G_c^l} \quad (7)$$

$$E_c^u = \frac{9K_c^u G_c^u}{3K_c^u + G_c^u} \quad (8)$$

The bounds on the Poisson's ratio as modified by Zimmerman are [38]

$$\nu_c^l = \frac{3K_c^l - 2G_c^u}{6K_c^l + 2G_c^u} \quad (9)$$

$$\nu_c^u = \frac{3K_c^u - 2G_c^l}{6K_c^u + 2G_c^l} \quad (10)$$

The lower and upper bounds are established with the softer and harder phases as the matrix respectively. The H–S model has received wide popularity [8,11,52,59–61,67]; however, Ravichandran suggested that the model could only apply to the composite system with small difference in elastic constants [8].

2.3. Ravichandran's bounds

Ravichandran modified the iso-strain and iso-stress unit cell to propose a unit cell, as shown in Fig. 1(d), composing of a continuous matrix and isolated particles [8]. He suggested that the elastic properties of the unit cell could be expressed as

$$E_C^l = \frac{(\boldsymbol{C}E_m E_p + E_m^2)(1 + \boldsymbol{C})^2 - E_m^2 + E_p E_m}{(\boldsymbol{C}E_p + E_m)(1 + \boldsymbol{C})^2} \quad (11)$$

$$E_C^u = \frac{[E_p E_m + E_m^2(1 + \boldsymbol{C})^2 - E_m^2](1 + \boldsymbol{C})}{(E_p - E_m)\boldsymbol{C} + E_m(1 + \boldsymbol{C})^3} \quad (12)$$

$$\nu_C^l = \frac{1}{(1 + C)^2}\left[\frac{(\nu_p E_m + C\nu_m E_p)}{(\boldsymbol{C}E_p + E_m)} + \nu_m(1 + C)^2 - \nu_m\right] \quad (13)$$

$$\nu_C^u = \frac{\nu_p E_m + C\nu_m E_p + E_m\nu_m(2C + 3C^2 + C^3)}{\boldsymbol{C}E_p + E_m(1 + 2C + 3C^2 + C^3)} \quad (14)$$

Table 1
Elastic properties of the constituent phase in the ceramic–metal composites

	Elastic modulus/GPa	Poisson's ratio
Al_2O_3	401	0.24
NiAl	186	0.31
SiC	450	0.22
Al	70	0.34
WC	700[a]	0.19
Co	207	0.31
Glass[b]	81	0.20
W	355	0.24

[a] Extrapolated from the values of WC–Co composites [4].
[b] A borosilicate glass.

where

$$\boldsymbol{C} = \left[\frac{1}{V_p}\right]^{1/3} - 1 \quad (15)$$

Ravichandran suggested that his model was suitable for the two-phase system with very different elastic constants [8], and has successfully verified it by comparing with several experimental data sets. However, his model failed to predict the Poisson's ratio of WC–Co and polymer–glass systems.

3. Experimental data

The experimental data of four ceramic–metal systems, Al_2O_3–NiAl, SiC–Al, WC–Co and glass–W, are compiled in the present study. These four systems are prepared by using the conventional powder processing technique, so these composites can be categorized as particulate composites. The elastic properties of these composites thus show little dependence on orientation. The properties of the constituent phase in these four systems are listed in Table 1. The elastic constants are mainly determined either by static methods [15], such as the measurement of longitudinal deformation, or by dynamic methods [39,40], such as the method by applying ultrasonic waves. The dynamic method can determine the elastic constants and Poisson's ratio at the same time. The static methods usually reported only elastic modulus due to the difficulties involved in the measurement of the transverse strain [3].

3.1. Al_2O_3–NiAl system

The Al_2O_3 content in the Al_2O_3–NiAl composites varies from 0 to 100% [6]. This system is the only ceramic–metal system that the reported elastic constants cover the full composition range. The composites were prepared by hot pressing at a temperature of 1450° C, which was lower than the melting points of the two constituents. Both Al_2O_3 and NiAl are continuous phases from 30%Al_2O_3 to 70%Al_2O_3. The Al_2O_3 and NiAl are weakly bonded together [6]; furthermore, no reaction phase at the interface was observed [41].

3.2. SiC–Al system

The SiC–Al composites were prepared by raising the processing temperatures above the melting point of Al alloy; however, SiC remains in its solid state [40,42–53]. The SiC particles are thus not strongly bonded together due to the processing temperature is far too low to result in sintering between SiC particles. Most the SiC content in the data collected from various literatures varies from 5 to 60%, a handful data from 60 to 74%. The wetting of Al melt on SiC is rather poor [54–56]. The surface of SiC particles is frequently coated with another phase to improve its wettability. The coated material may dissolve into Al matrix to form alloy. To avoid the complexity of choosing datum for Al matrix, only the data without the coating are reported in the present study.

3.3. WC–Co system

The wetting angle of Co melt on WC is low for their mutual solubility [57]. The WC–Co composites are prepared by a liquid phase sintering route [58–61]. The WC content in the reported literature varies mainly between from 50 to 98%. Only three data points vary from 10 to 35%. It may be due to the fact that the specimen shape may be seriously distorted as the Co amount is too high.

3.4. Glass–W system

Different from the above systems, the elastic modulus of the metal W is higher than that of ceramic in the glass–W composite [62]. The W particles are spherical in shape and the wetting angle of the borosilicate glass on W is low [63]. The glass amount in the composites varies from 50 to 90%. Most W particles are isolated to each other within the glass matrix.

4. Comparison

4.1. Elastic modulus of ceramic–metal composites

Fig. 2 shows all the available experimental data on the elastic modulus of the ceramic–metal systems as a function of ceramic content. The Voigt–Reuss bounds are shown in the figure for comparison. The Voigt–Reuss bounds are close to each other as the elastic moduli of the two phases in the composite are similar in values, such as the cases of Al_2O_3–NiAl composites. Therefore, the experimental data of the composites are close to the prediction made by the rule of mixtures [Eq. (1)]. However, for other composites with two phases of different elastic modulus, such as SiC–Al and WC–Co composites, the upper and lower bounds are widely apart. In any case, all the experimental data of the ceramic–metal composites fall within the Voigt–Reuss bounds.

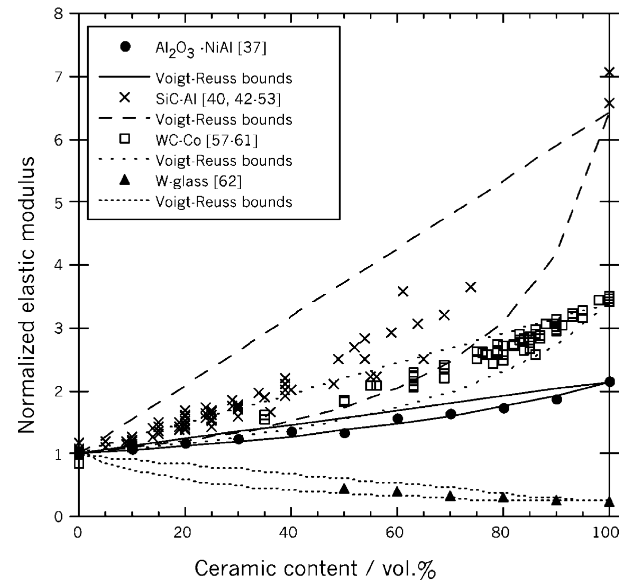

Fig. 2. Normalized elastic moduli of the ceramic–metal composites as function of ceramic content. The Voigt–Reuss bounds are shown for comparison.

Fig. 3 shows the comparison between the experimental data and the H–S bounds. Most experimental data also fall within the H–S bounds. Since the H–S bounds are relatively closer to each other than those of the Voigt–Reuss bounds, the H–S model offers closer bounds on the estimation of elastic moduli for ceramic–metal composites.

Fig. 4 shows the comparison between the experimental data and the Ravichandran bounds. Though the Ravichandran bounds are the closest pairs among three pairs; many experimental data fall outside the bounds.

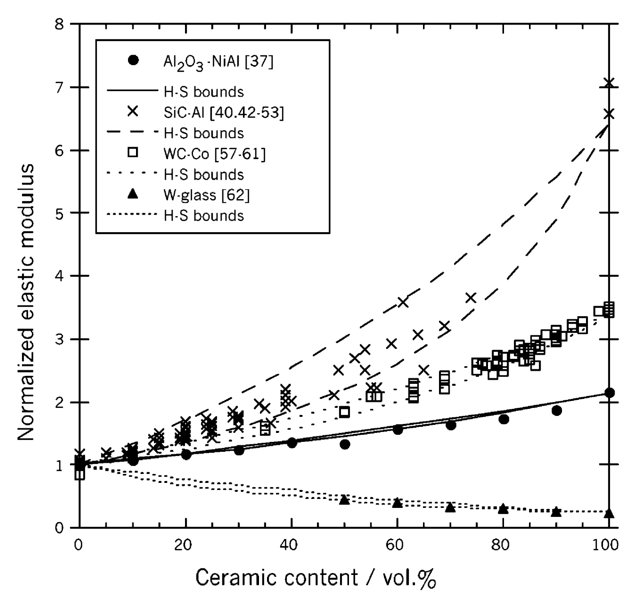

Fig. 3. Normalized elastic moduli of the ceramic–metal composites as function of ceramic content. The H–S bounds are shown for comparison.

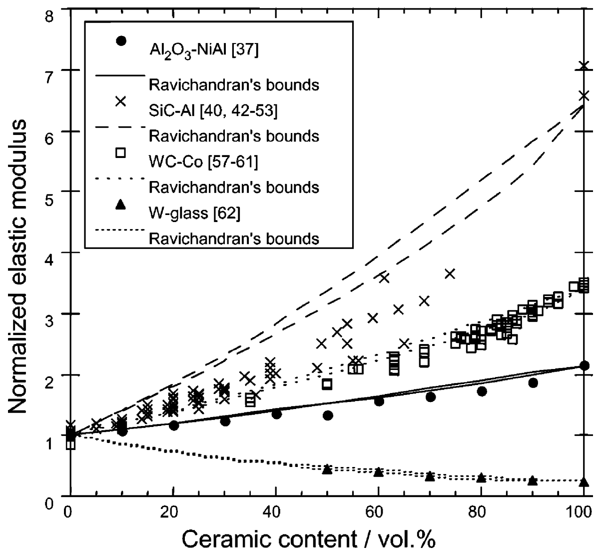

Fig. 4. Normalized elastic moduli of the ceramic–metal composites as function of ceramic content. The Ravichandran's bounds are shown for comparison.

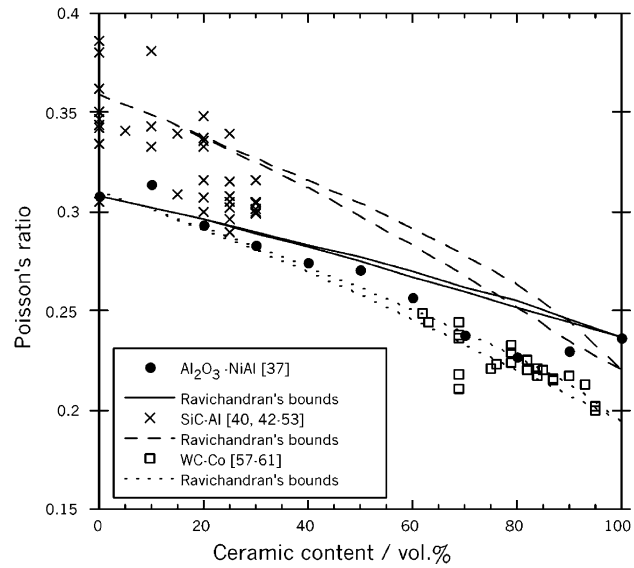

Fig. 6. Poisson's ratio of the ceramic–metal composites as function of ceramic content. The Ravichandran's bounds are shown for comparison.

4.2. Poisson's ratios of ceramic–metal composites

The experimental data collected from various literatures are shown in Fig. 5. The reported data on the Poisson's ratio are much less than those of the elastic modulus. The experimental data on Poisson's ratio for the SiC–Al and WC–Co systems cover only a small composition range, from 5 to 30% SiC for the SiC–Al system and from 63 to 95% WC for WC–Co system, as shown in Fig. 5. The only experimental data set covering the whole composition range is the data set of the Al_2O_3–NiAl system. Furthermore, the data for the SiC–Al system scatter significantly even when the composition is the same.

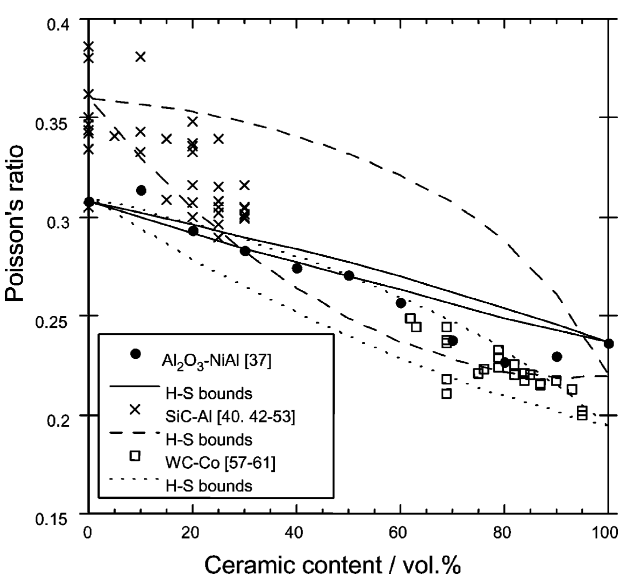

Fig. 5. Poisson's ratio of the ceramic–metal composites as function of ceramic content. The H–S bounds are shown for comparison.

Fig. 5 shows the comparison between the experimental data of Poisson's ratio and H–S bounds. The theoretical bounds are close to each other as the difference between the Poisson's ratios of the two phases in the composite is smaller, as the case of the Al_2O_3–NiAl composites. Most experimental data of SiC–Al and WC–Co composites fall within the H–S bounds. However, the experimental data of the Al_2O_3–NiAl composite with low second-phase concentration fall outside of the bounds. Comparison is also made between the experimental values and Ravichandran's bounds (Fig. 6). Though Ravichandran bounds are the closest pair, many experimental data fall outside the bounds.

5. Discussion

The Voigt–Reuss model treats a laminated system. Each layer (phase) in the system is separated by another layer (phase). The microstructure of the particulate composites is very much different from those shown in Fig. 1(a) and (b). The H–S and Ravichandran models treats the system composing a continuous matrix and an isolated phase, Fig. 1(c) and (d). The interactions between each strain field around one particle are assuming none or negligible. Therefore, strictly speaking, the H–S and Ravichandran models should apply to the system with low second-phase concentration. Nevertheless, the elastic moduli of all ceramic–metal systems collected in the present study fall within the Voigt–Reuss and H–S bounds.

In the WC–Co composites, the metallic Co matrix separates the WC particles from each other. The SiC particles are not sintered together in the SiC–Al composite. Most metallic particles are isolated within the glassy matrix in the glass–W composites. Therefore, the microstructure of WC–Co, SiC–Al and glass–W systems is close to the one assumed in the H–S model. However, both phases are continuous as Al_2O_3 content varies from 30 to 70% in the Al_2O_3–NiAl composites [37]. The two phases in the composites within this composition range form an interpenetrating microstructure; which is quite different from that of SiC–Al, WC–Co and glass–W system. However, the Voigt–Reuss and H–S bounds can be applied to estimate the elastic modulus of the composites with interpenetrating microstructure. It demonstrates that the models on elastic modulus show little dependence on microstructure features.

The Ravichandran model shows closest bounds; however, the bounds fail to describe the elastic moduli of most ceramic–metal particulate composites. It suggests that the model is sensitive to microstructural variation.

The Poisson's ratio of the SiC–Al and WC–Co composites and the Al_2O_3–NiAl composites with interpenetrating microstructure falls within the H–S model, Fig. 5. However, the Poisson's ratios of the Al_2O_3-rich and NiAl-rich Al_2O_3–NiAl composites fall outside the H–S bounds.

Though the Poisson's ratio of WC–Co system falls within the H–S bounds, it should be noted that fully dense WC could not be prepared without the presence of liquid Co phase. The Poisson's ratio for pure WC is calculated by extrapolating the experimental data of WC–Co composites to 100% WC [4]. It may lead to the underestimation of the value for pure WC. For the SiC–Al composites, Al matrix is always alloyed with other elements. The reported values on the Poisson's ratios of Al-matrix alone scatter significantly, Fig. 5. It results in difficulties of estimating the H–S bounds for the composites. An average value of all the data for Al-matrix was used, uncertainty thus exists near the Al-rich side composition. Therefore, more attention should be given to the comparison between the model prediction and the experimental data of Al_2O_3–NiAl system.

The theoretical predictions fail to describe the Poisson's ratio of the Al_2O_3–NiAl composites with only one continuous phase, Fig. 5. From the figure, it is noted that the Poisson's ratio of the composites is similar to that of the monolithic materials as a small amount of second phase is added into the matrix. Contrary to the assumption adopted by most theoretical models [16–38], the Al_2O_3 and NiAl are not bonded perfectly. The interface is relatively weak instead [41]. As a load is applied on the composite with the presence of weakly bonded isolated particles, the load is mainly sustained by the matrix alone. The strains along and perpendicular to the loading direction are thus close to those of matrix alone. In other words, the existence of the second phase affects little to the strain of the matrix. The composite thus responds to the external load as if no second phase is present at all; so the Poisson's ratio of the composites remains more or less the same. However, as the two phases form an interpenetrating microstructure, one phase is closely constrained by the other one though they do not bond strongly together. The elastic behavior of the matrix is thus affected by the presence of the interpenetrating second phase. The Poisson's ratio of the composite with interpenetrating microstructure then follows the theoretical predictions for two-phase materials.

The deviation between experimental data and theoretical predictions is frequently attributed to the microstructural complexity of real composites in previous studies [13,64–68]. Therefore, some theoretical models employed numerical analysis, included the finite element or boundary element methods to adopt the shape irregularity. However, to the best of our knowledge, none of the theoretical models has ever taken the interconnectivity and interface characteristics into account. It may have something to do with the fact that a data set that covers full composition range was not previously available. It is also noted that the Al_2O_3–NiAl system is the only system that is sintered at its solid state. The Al_2O_3–NiAl interface is weakly bonded [41]. The presence of weak interface may render the existence of the continuous skeleton more influential. In any case, it suggests that unlike the case for elastic modulus, the Poisson's ratio depends strongly on the microstructural characteristics. Furthermore, it indicates that there are needs on the analysis of the Poisson's ratio for two-phase material. Though attempt has been made to analyze the deviation as a function of microstructure characteristics, no progress can be reported at this stage.

6. Conclusions

The comparison between experimental data on elastic constants and several model predictions is made in the present study. The experimental data cover the full composition range of ceramic–metal composites. The model predictions offer upper and lower bounds to compensate the scatter of the data. The following conclusions can be drawn from the present study.

(1) The elastic modulus of the ceramic–metal composites can be described by using Voigt–Reuss bounds and H–S bounds. However, the H–S bounds are relatively closer to each other.
(2) The Voigt–Reuss and H–S bounds on elastic moduli show little dependence on the microstructural characteristics of ceramic–metal composites.

For the Poisson's ratio of the ceramic–metal composites, the following conclusions can be made.

(1) The Poisson's ratio of the composites shows strong dependence on microstructural characteristics.
(2) The interconnectivity of each phase in a composite may affect the value of Poisson's ratio of composites.
(3) The bonding characteristics of interface may also affect the Poisson's ratio of composites.

Acknowledgments

The National Science Council, R.O.C., supported the present work through the contract of NSC86-2216-E002-023.

References

[1] R. Morrell, Handbook of Properties of Technical and Engineering Ceramics, HMSO, London, 1987.
[2] H. Ledbetter, S. Kim, D. Balzar, S. Crudele, W. Kriven, J. Am. Ceram. Soc. 81 (1998) 1025.
[3] W. Koester, H. Franz, Metall. Rev. 6 (1961) 1.
[4] H. Doi, Y. Fujiwara, K. Miyake, Y. Oosawa, Metall. Trans. 1 (1970) 1417.
[5] M.F. Ashby, Acta Metall. Mater. 41 (1993) 1313–1335.
[6] W.H. Tuan, Y.P. Pai, J. Am. Ceram. Soc. 82 (1999) 1624–1626.
[7] S.M. Barinov, V. Yu Evdokimov, Acta Metall. Mater. 41 (1993) 801.
[8] K.S. Ravichandran, J. Am. Ceram. Soc. 77 (1994) 1178.
[9] M. Saski, T. Hirai, J. Ceram. Soc. Jp. 99 (1991) 770.
[10] D.P. Miller, J.J. Lannutti, J. Mater. Res. 8 (1993) 2004.
[11] J.R. Zuiker, Compd. Eng. 7 (1995) 807.
[12] A. Kawasaki, R. Watanabe, Ceram. Int. 23 (1997) 73.
[13] M.M. Gasik, Compd. Mater. Sci. 13 (1998) 42.
[14] K.K. Chawla, Ceramic Matrix Composites, Chapman & Hill, New York, 1993.
[15] M.F. Ashby, D.R.H. Jones, Engineering Materials 1—An Introduction to their Properties and Applications, Pergamon Press, Oxford, 1980.
[16] W. Voigt, Ann. Phys. 38 (1889) 573.
[17] A. Reuss, Z. Angrew. Math. Mech. 9 (1929) 49.
[18] B. Paul, Trans. AIME 218 (1960) 36.
[19] Z. Hashin, S. Shtrikman, J. Mech. Phys. Solids 10 (1962) 335.
[20] Z. Hashin, S. Shtrikman, J. Mech. Phys. Solids 10 (1962) 343.
[21] Z. Hashin, S. Shtrinkman, J. Mech. Phys. Solids 11 (1963) 127.
[22] R. Hill, J. Mech. Phys. Solids 11 (1963) 357.
[23] B. Budiansky, J. Mech. Phys. Solids 13 (1965) 223.
[24] T.T. Wu, J. App. Mech. 32 (1965) 211.
[25] T.T. Wu, Int. J. Solid Struct. 2 (1966) 1.
[26] T.G. Richard, J. Compd. Mater. 9 (1975) 108.
[27] J.C. Halpin, J.L. Kardos, Poly. Eng. Sci. 16 (1976) 344.
[28] J.P. Watt, G.F. Davies, R.J. O'Connell, Rev. Geophys. Space Phys. 14 (1976) 541.
[29] Y. Benveniste, Mech. Mater. 6 (1987) 147.
[30] J.P. Matt, Phys. Chem. Min. 15 (1988) 579.
[31] M.F. Ashby, Acta Metal. Mater. 40 (1993) 1313.
[32] L.J. Walpole, J. Mech. Phys. Solids 14 (1966) 155.
[33] R.H.T. Yen, J. App. Phys. 42 (3) (1971) 1101.
[34] G.W. Milton, N. Phan-Thien, Proc. R. Soc. London A380 (1982) 305.
[35] G.W. Milton, J. Mech. Phys. Solids 30 (1982) 177.
[36] Z. Hashin, J. App. Mech. 50 (1983) 481.
[37] C.L. Hsieh, W.H. Tuan, J. Euro. Ceram. Soc. 24 (2004) 3789.
[38] R.W. Zimmerman, Mech. Res. Commun. 19 (1992) 563.
[39] P.K. Liaw, D.K. Hsu, N. Yu, N. Miriyala, V. Sain, H. Jeong, Acta Mater. 44 (1996) 2101.
[40] Y. Lu, P.K. Liaw, J. Compd. Mater. 29 (1995) 1096.
[41] W.H. Tuan, W.B. Chou, H.C. You, S.T. Chang, Mater. Chem. Phys. 56 (1998) 157.
[42] D.J. Lloyd, Int. Mater. Rev. 39 (1) (1994) 1.
[43] M. Sherif El-Eskandarany, J. Alloys Compd. 279 (1998) 263.
[44] P.K. Liaw, R.E. Shannon, W.G. Vlark Jr., W.C. Harrigan Jr., H. Jeong, D.K. Hsu, Mater. Chem. Phys. 39 (1995) 220.
[45] D.L. McDanels, Metall. Trans. A 16A (1985) 1105.
[46] C.R. Crowe, R.A. Gray, D.F. Hasson, in: W.C. Harrigan Jr., J. Strife, A.K. Dhingra (Eds.), Microstructure Controlled Fracture Toughness, in ICCM-V, The Metallurgical Society, Inc., 1985, p. 843.
[47] W.R. Hoover, in: Proceedings of an International Conference on Fabrication of Particulates Reinforced Metal Composites, Am. Soc. Metals, Metals Park, OH, 1990, p.115.
[48] I.A. Ibrahim, F.A. Mohamed, E.J. Lavernia, J. Mater. Sci. 26 (1991) 1137.
[49] A. Mortensen, in: Proceedings of an International Conference on Fabrication of Particulates Reinforced Metal Composites, Am. Soc. Metals, Metals Park, OH, 1990, p.217.
[50] M.K. Premkumar, W.H. Hunt Jr., R.R. Sawtell, J. Met. 44 (1992) 24.
[51] C. Zweben, J. Met. 44 (1992) 15.
[52] G. Mott, P.K. Liaw, Metall. Trans. 19A (1988) 2233.
[53] M. Orrhede, R. Tolani, K. Salama, Res. Nondestruct. Eval. 8 (1996) 23.
[54] V. Laurent, C. Rado, N. Eustathopoulos, Mater. Sci. Eng. A205 (1996) 1.
[55] V. Laurent, D. Chatain, N. Eustathopoulos, J. Mater. Sci. 22 (1987) 244.
[56] A.C. Ferro, B. Derby, Acta Metall. Mater. 43 (8) (1995) 3061.
[57] P. Harmat, I. Kotsis, L. Laczko, L. Bartha, Solid State Ion. 141-142 (2001) 157.
[58] H. Doi, Y. Fujiwara, K. Miyake, Y. Oosawa, Metall. Trans. 1 (1970) 1417.
[59] P. Kwon, C.K.H. Dharan, Acta Metall. Mater. 43 (3) (1995) 1141.
[60] Z. Fan, A.P. Miodownik, P. Tsakiropoulos, Mater. Sci. Tech. 9 (1993) 1094.
[61] M. Sherif El-Eskandarany, A.A. Mahday, H.A. Ahmed, A.H. Amer, J. Alloys Compd. 312 (2000) 315.
[62] D.P.H. Hasselman, R.M. Fulrath, J. Am. Ceram. Soc. 48 (10) (1965) 548.
[63] C.Y. Haein, J. Schroers, W.L. Johnson, Appl. Phys. Lett. 80 (11) (2002) 1906.
[64] Y.-L. Shen, M. Finot, A. Needleman, S. Suresh, Acta Metall. Mater. 42 (1994) 77.
[65] J. Mackerle, Finite Elements, Anal. Des. 38 (2002) 567.
[66] E.J. Garboczi, A.R. Day, J. Mach. Phys. Solids 43 (1995) 1349.
[67] H.S. Kim, S.I. Hong, S.J. Kim, J. Mater. Proc. Tech. 112 (2001) 109.
[68] A.P. Roberts, E.J. Garbozi, J. Mech. Phys. Solids 47 (1999) 2029.